



This is the accepted manuscript made available via CHORUS, the article has been published as:

Successive Phase Transitions and Extended Spin-Excitation Continuum in the $S=1/2$ Triangular-Lattice Antiferromagnet $\text{Ba}_3\text{CoSb}_2\text{O}_9$

H. D. Zhou, Cenke Xu, A. M. Hallas, H. J. Silverstein, C. R. Wiebe, I. Umegaki, J. Q. Yan, T. P. Murphy, J.-H. Park, Y. Qiu, J. R. D. Copley, J. S. Gardner, and Y. Takano

Phys. Rev. Lett. **109**, 267206 — Published 26 December 2012

DOI: [10.1103/PhysRevLett.109.267206](https://doi.org/10.1103/PhysRevLett.109.267206)

Successive phase transitions and extended spin-excitation continuum in the $S=\frac{1}{2}$ triangular-lattice antiferromagnet $\text{Ba}_3\text{CoSb}_2\text{O}_9$

H. D. Zhou,^{1,2,*} Cenke Xu,³ A. M. Hallas,⁴ H. J. Silverstein,⁴ C. R. Wiebe,^{2,4,5} I. Umegaki,⁶ J. Q. Yan,^{7,8} T. P. Murphy,² J.-H. Park,² Y. Qiu,^{9,10} J. R. D. Copley,⁹ J. S. Gardner,^{9,11} and Y. Takano¹²

¹*Department of Physics and Astronomy, University of Tennessee, Knoxville, Tennessee 37996-1200, USA*

²*National High Magnetic Field Laboratory, Florida State University, Tallahassee, Florida 32306-4005, USA*

³*Department of Physics, University of California, Santa Barbara, California 93106, USA*

⁴*Department of Chemistry, University of Manitoba, Winnipeg, Manitoba, R3T 2N2 Canada*

⁵*Department of Chemistry, University of Winnipeg, Winnipeg, Manitoba, R3B 2E9 Canada*

⁶*Department of Physics, Tokyo Institute of Technology, Meguro, Tokyo 152-8551, Japan*

⁷*Materials Science and Technology Division, Oak Ridge National Laboratory, Oak Ridge, Tennessee 37831, USA*

⁸*Department of Materials and Engineering, University of Tennessee, Knoxville, Tennessee 37996, USA*

⁹*NIST Center for Neutron Research, Gaithersburg, Maryland 20899-6102, USA*

¹⁰*Department of Materials Science and Engineering,
University of Maryland, College Park, Maryland 20742, USA*

¹¹*Indiana University, Bloomington, Indiana 47408, USA*

¹²*Department of Physics, University of Florida, Gainesville, Florida 32611-8440, USA*

(Dated: November 13, 2012)

Using magnetic, thermal, and neutron measurements on single-crystal samples, we show that $\text{Ba}_3\text{CoSb}_2\text{O}_9$ is a spin-1/2 triangular-lattice antiferromagnet with the c axis as the magnetic easy axis and two magnetic phase transitions bracketing an intermediate up-up-down phase in magnetic field applied along the c axis. A pronounced, extensive neutron-scattering continuum above spin-wave excitations, observed below T_N , implies that the system is in close proximity to one of two spin-liquid states that have been predicted for a 2D triangular lattice.

PACS numbers: 75.40.Cx, 75.45.+j, 75.40.Gb, 78.70.Nx

The two-dimensional (2D) triangular-lattice antiferromagnet (TAF) is one of the simplest possible geometrically frustrated systems. When the spin is small, especially $S = 1/2$, strong quantum fluctuations in this magnet can lead to exotic quantum ground states. One example of such states is the quantum spin liquid (QSL), in which the spin ensemble is prevented from ordering by quantum fluctuations and remains in a disordered, liquid-like state [1]. Although Anderson has proposed in 1973 the resonating-valence-bond state, one kind of QSL [2], it is only recently that several spin-1/2 TAFs—notably κ -(BEDT-TTF)₂Cu₂(CN)₃ [3, 4], and EtMe₃Sb[Pd(dmit)₂]₂ [5, 6]—have been established as QSL candidates. Cs₂CuCl₄ is another spin-1/2 TAF that has been related to a QSL, although it orders at about 0.6 K. Inelastic-neutron-scattering continua in this material have been attributed to the proximity of the system to a QSL, in which spin-wave excitations are fractionalized into spin-1/2 spinons [7, 8].

A second example of exotic magnetism in TAFs is the novel up-up-down (uud) ground state, predicted to be stabilized in spin-1/2 TAFs by quantum fluctuations [9–11]. This state manifests itself as a constant magnetization, equal to 1/3 of the saturation magnetization M_s , over a finite field range. Cs₂CuBr₄ is a rare example of a spin-1/2 TAF in which an uud state occurs with an $M_s/3$ magnetization plateau [12, 13]. Recently, such a plateau has also been found in another spin-1/2 TAF, $\text{Ba}_3\text{CoSb}_2\text{O}_9$ [14]. The crystal structure of this

6H perovskite, with lattice constants $a = b = 5.8562 \text{ \AA}$ and $c = 14.4561 \text{ \AA}$, can be represented as a framework consisting of corner-sharing CoO₆ octahedra and face-sharing Sb₂O₉ bi-octahedra, as shown in Fig. 1(a). The Co²⁺ ions, which occupy the 2a Wyckoff sites of space group P6₃/mmc, form triangular lattices parallel to the ab plane (Fig. 1(b)), separated by double layers of non-magnetic Sb. Weak interlayer interactions cause the system to order at about 3.8 K [14, 15]. Due to the strong spin-orbit coupling and a uniaxial crystal field, the ground state of Co²⁺ ions in $\text{Ba}_3\text{CoSb}_2\text{O}_9$ is a Kramers doublet with $l^z + S^z = \pm 1/2$. Therefore, at low temperatures the material can be described as a TAF with an effective spin 1/2 [14, 15].

Until now, studies of $\text{Ba}_3\text{CoSb}_2\text{O}_9$ have been largely limited to polycrystalline samples. The dearth of single-crystal experiments has left several questions open: (i) To what extent is the material isotropic? (ii) How does the magnetic field influence the magnetic ordering, and what is the magnetic phase diagram? In most antiferromagnetic Mott insulators, the Heisenberg coupling J is too high (on the order of 100 K \sim 1000 K) compared with a magnetic field that can be achieved in the laboratory, thus little of the material property is changed in magnetic field. On the other hand, if the Heisenberg coupling is too weak, then it is difficult to reach a low enough temperature to probe the quantum ground state of the system. One of the great advantages of $\text{Ba}_3\text{CoSb}_2\text{O}_9$ is that its J ($\sim 18 \text{ K}$ [14]) is at a very appropriate scale:

not too large but large enough so that temperatures two orders of magnitude lower than it can be reached in the laboratory. Thus the phase diagram of this material in magnetic field can be fully explored in the laboratory. (iii) Whether the system is close to a spin-liquid phase, although it does order at about 3.8 K.

In this letter, we report results of magnetic, specific-heat, and neutron-scattering measurements on single crystals of $\text{Ba}_3\text{CoSb}_2\text{O}_9$, uncovering successive magnetic phase transitions bracketing an intermediate udd phase in magnetic fields applied along the c axis, which we find to be the easy axis. Moreover, a broad continuum above the spin-wave excitations, observed at 1.5 K, implies that the system is in close proximity to a spin-liquid phase on a 2D triangular lattice.

Single crystals of $\text{Ba}_3\text{CoSb}_2\text{O}_9$ were grown by the traveling-solvent floating-zone technique. The X-ray Laue diffraction was used to orient the crystal. DC susceptibility and magnetization were measured by a vibrating sample magnetometer, and magnetic torque was measured by using a 13 μm -thick CuBe cantilever. The specific-heat measurements were performed in two setups: a Physical Properties Measurements System for $\mu_0 H \leq 9$ T and a home-built relaxation calorimeter for higher fields up to 18 T. The neutron-scattering measurements were performed with $\lambda = 4.8$ Å, on the Disk Chopper Spectrometer at NIST.

Neutron-diffraction intensities at 1.5 K in zero magnetic field, after subtracting those at 40 K, show magnetic peaks at the wave vector $(\frac{1}{3}, \frac{1}{3}, 1)$ and multiples, indicative of a 120° spin structure, as shown in Fig. 1(c). This is in agreement with an earlier result on a polycrystalline sample [15]. The magnetic susceptibility, $\chi = M/H$, at 5 T exhibits a peak at about 3.6 K, corresponding to the reported antiferromagnetic ordering [14, 15], when $H//c$, but not when $H//a$ (Fig. 1(d)). At 2 K, the magnetization up to 9 T rises more rapidly with increasing field for $H//c$ than for $H//a$ (inset of Fig. 1(d)). This anisotropy persists even after the magnetization and field are scaled, indicating that it does not arise from an anisotropy in the g factor alone. These results clearly show that the c axis is the magnetic easy axis.

With increasing field, the χ peak for $H//c$ moves to lower temperatures, as shown in Fig. 2(a). At 6 T, an additional feature, a slope change, appears at about 4 K and moves to higher temperatures with increasing field. Accordingly, the derivative $d(\chi T)/dT$ exhibits one anomaly at low fields and two anomalies at high fields, as shown in Fig. 2(b) for $\mu_0 H = 3$ T and 8 T. We define T_{N1} and T_{N2} by the locations of the lower- and higher-temperature anomalies, respectively. The magnetic torque at 27 mK (Fig. 1(e)) exhibits two clear anomalies, at $\mu_0 H_{c1} = 9.8$ T and $\mu_0 H_{c2} = 15.1$ T parallel to the c axis.

Specific heat, C_P , for $H//c$ is shown in Figs. 2(c)–2(e). The zero-field data, at temperatures in increments of 0.01 K, show a single peak at T_{N1} . With increasing

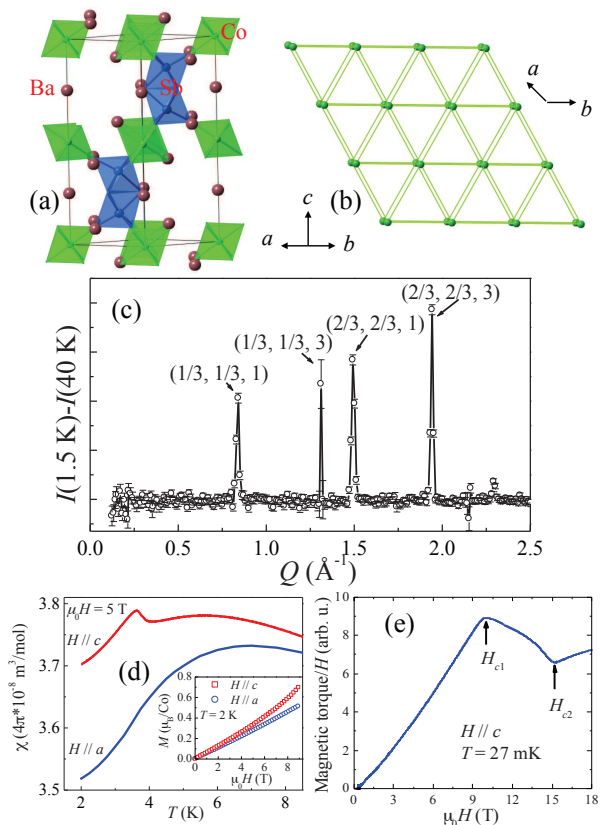


FIG. 1: (Color online) (a) Schematic crystal structure of $\text{Ba}_3\text{CoSb}_2\text{O}_9$. Green octahedra represent Co sites and blue octahedra represent Sb sites. (b) Magnetic lattice composed of Co^{2+} ions. (c) Neutron-diffraction data at 1.5 K, after subtracting the 40 K data. The error bars represent $\pm 1\sigma$. (d) Temperature dependences of the magnetic susceptibility, χ , at 5 T. Inset: Magnetization at 2 K. (e) Torque in magnetic fields $H//c$ at 27 mK.

field, this peak becomes smaller and moves to lower temperatures. At 5.8 T, another peak appears at a higher temperature, which is consistent with T_{N2} determined from χ . As shown in Fig. 2(b), both $d(\chi T)/dT$ and C_P/T show one feature, at T_{N1} , at 3 T and two features, at T_{N1} and T_{N2} , at 8 T. With increasing field, this second peak grows and moves to higher temperatures, and reaches a maximum at about 12 T, above which it decreases in height and temperature. C_P as a function of field, measured with a fixed electric current to a heater attached to the thermal reservoir, shows that H_{c1} decreases, whereas H_{c2} increases, with increasing temperature (Fig. 2(e)). By contrast, C_P measured in $H//a$ at 9 T, exhibiting a single peak, is similar to that at zero field except for a small shift of the peak to a lower temperature (Fig. 2(f)).

All the transition features described above are used to construct the T – H phase diagram for $H//c$ shown in Fig. 3. Three regions (A–C) are identified. In region

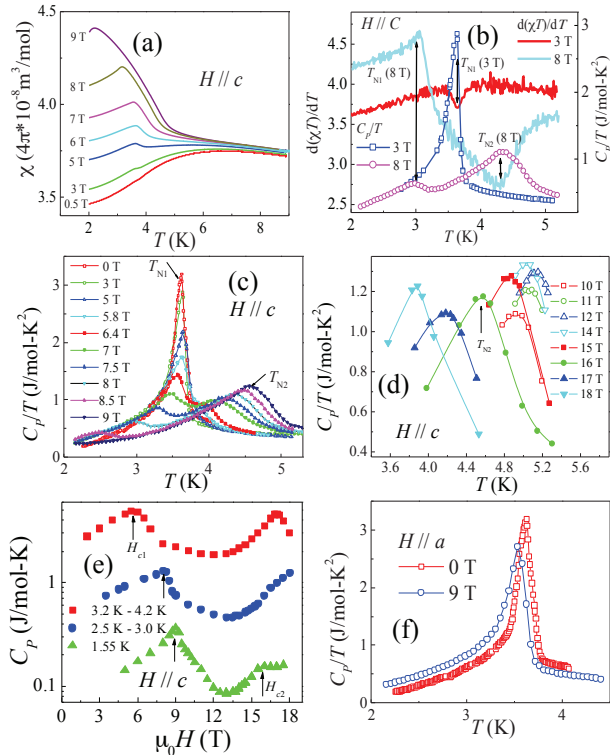


FIG. 2: (Color online) (a) Temperature dependence of χ of $\text{Ba}_3\text{CoSb}_2\text{O}_9$ at different fields $H//c$. (b) $d(\chi T)/dT$ vs. T and C_P/T vs. T at 3 T and 8 T with $H//c$. (c and d) Temperature dependence of C_P/T at different fields $H//c$. (e) Specific heat for $H//c$ as a function of field. (f) Specific heat at 9 T applied along the a axis, along with the zero-field data for comparison.

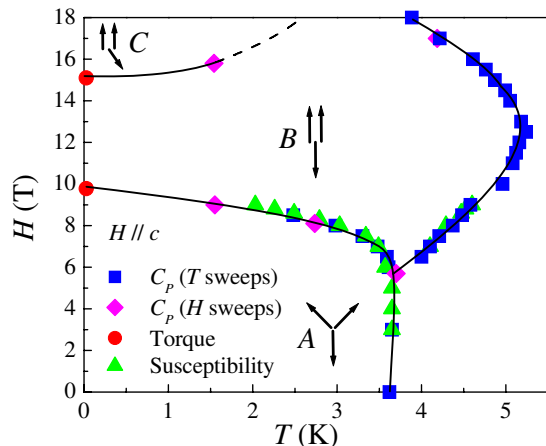


FIG. 3: (Color online) Magnetic phase diagram of $\text{Ba}_3\text{CoSb}_2\text{O}_9$ for $H//c$. A : 120° structure phase, B : uud phase, C : oblique phase. The arrows represent the spin structures in each phase.

A , a 120° structure with spins canting toward the c axis due to easy-axis anisotropy is stable. With increasing H , the uud structure takes over in the intermediate region B , leading to a $1/3$ magnetization plateau, as has been confirmed by magnetization measurements on a powder sample [14]. With further increase in H , the uud structure gives way to the “oblique” structure (region C) with two parallel spins and one canted to a different direction.

It is noteworthy that our zero-field specific heat, measured in 0.01 K increments, shows only one transition, indicating that the uud phase is stable only at finite fields. Near and at zero field, the phase diagram of the triangular-lattice antiferromagnet is not yet fully understood even for classical spins, let alone $S=1/2$. For a Heisenberg model with an easy-axis exchange anisotropy, the uud phase has been predicted to extend to $H=0$ [16, 17], and an easy-axis single-ion anisotropy has been shown to stabilize uud-like phases at $H=0$ [18]. By contrast, the uud phase appears to be either absent or very narrow at $H=0$ for the isotropic Heisenberg model [19–21]. Relying on these predictions for classical spins, we propose that $\text{Ba}_3\text{CoSb}_2\text{O}_9$ is close to the isotropic Heisenberg model, despite the evidence that it has a magnetic easy axis, the c axis. Recently reported zero-field specific heat $a\text{Ba}_3\text{CoSb}_2\text{O}_9$ crystal grown from a melt shows a three-step transition over a very narrow temperature range, about 3% of T_{N1} [14]. As in our case, this narrowness has been interpreted to indicate that the system is close to the isotropic Heisenberg model. The discrepancy in the number of transition steps between our result and that of Ref. [14] is probably attributable to the difference in the reported-growth techniques.

The reported saturation field of $\text{Ba}_3\text{CoSb}_2\text{O}_9$ is $\mu_0 H_{c3} = 31.9$ T [14]. Therefore, the width of the uud phase determined here at 27 mK is $0.16H_{c3}$, covering $0.31 \leq H/H_{c3} \leq 0.47$. This large width near zero temperature is consistent with powder-sample magnetization data at 1.3 K [14]. In a TAF with classical spins, thermal fluctuations stabilize the uud phase at finite temperatures. The magnetic field range of this thermally stabilized uud phase decreases with decreasing temperature and vanishes at zero temperature. Classical theory has predicted that both an easy-axis exchange anisotropy and an easy-axis single-ion anisotropy can make the uud phase survive down to zero temperature [17], as has been observed in $\text{Rb}_4\text{Mn}(\text{MoO}_4)_3$ with Mn^{2+} ($S=5/2$) [22]. However, $\text{Ba}_3\text{CoSb}_2\text{O}_9$ is close to the Heisenberg model with isotropic exchange interactions as argued above, and single-ion anisotropy does not exist for $S=1/2$. Therefore, the only other known stabilizing mechanism, quantum spin fluctuations [9, 23–25], must be mainly responsible for the large width of the uud phase near zero temperature in $\text{Ba}_3\text{CoSb}_2\text{O}_9$.

In this respect, the phase diagram of $\text{Ba}_3\text{CoSb}_2\text{O}_9$ is similar to that of Cs_2CuBr_4 . However, in Cs_2CuBr_4 , the triangular lattice is distorted, resulting in spatially

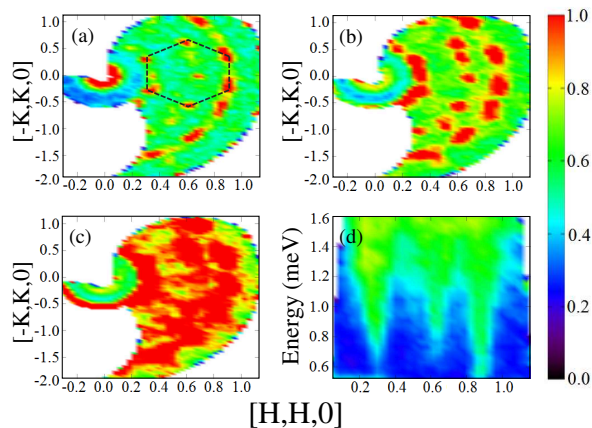


FIG. 4: (Color online) Intensity contour plots for inelastic neutron scattering at 1.5 K (a) For the energy range of 0.6–0.8 meV. (b) For 0.8–1.1 meV. (c) For 1.1–1.3 meV. Dashed lines in (a) indicate the three-sublattice Brillouine zones. (d) A cut along $[H,H,0]$ for K ranging from 0.2 to 0.5 reciprocal lattice units.

anisotropic nearest-neighbor exchange interactions with $J_2/J_1 = 0.74$ [12, 13]. Moreover, the phase boundaries of the uud phase in Cs_2CuBr_4 are first order as indicated by steps in magnetic torque data [13], probably due to a weak Dzyaloshinskii-Moriya interaction arising from the low lattice symmetry. By contrast, such steps are absent (Fig. 2(e)) in $\text{Ba}_3\text{CoSb}_2\text{O}_9$, indicating that the phase boundaries in this material are second order, as predicted for an ideal spin-1/2 Heisenberg TAF [9].

Figure 4 shows the inelastic neutron scattering pattern for $\text{Ba}_3\text{CoSb}_2\text{O}_9$ at 1.5 K. At this temperature, below T_{N1} , magnetic excitations are clearly observed (Fig. 4(d)). At low energy (Fig. 4(a)), spin-wave excitations appear, forming a hexagonal pattern. With increasing energy (Figs. 4(b) and 4(c)), these excitations expand to form a continuum. A cut along $[H,H,0]$ also shows clearly a broad continuum above the spin-wave dispersion at least up to 1.6 meV (Fig. 4(d)). The minima of the spin-wave excitations at the commensurate wave vector $\mathbf{Q}_0 = (\frac{1}{3}, \frac{1}{3}, 0)$ and its multiples is also observed (Fig. 4(d)). The continuum implies either strong interactions and scattering between spin-wave modes, or a strong fractionalization of spin-wave excitations. In Cs_2CuCl_4 , similar continua have been observed by inelastic neutron scattering [7, 8] and have been interpreted as the fractionalization of spin-wave excitations due to the quasi-one-dimensional nature of this material. However, fractionalization of spin-wave excitations in an isotropic 2D system has never been clearly observed previously. Since the triangular lattice in $\text{Ba}_3\text{CoSb}_2\text{O}_9$ is ideal, the continuum of Fig. 4 could be the first experimental evidence for fractionalization of spin-wave excitations in two

dimensions, implying that the spin order in $\text{Ba}_3\text{CoSb}_2\text{O}_9$ is in close proximity to a spin-liquid phase on the triangular lattice.

What type of spin-liquid state is this? Since this state is close to a spin order in which spin wave excitations have a clear minimum at the commensurate wave vector \mathbf{Q}_0 , it is reasonable to expect not only that the state has gapless fractionalized spinon excitations but also that its spin structure factor peaks at \mathbf{Q}_0 . So far three types of spin liquids have been proposed for 2D spin-1/2 TAFs such as $\kappa\text{-(ET)}_2\text{Cu}_2(\text{CN})_3$ and $\text{EtMe}_3\text{Sb}[\text{Pd}(\text{dmit})_2]_2$:

(i) A spinon Fermi-surface state with a fluctuating $U(1)$ gauge field [26, 27]. This state has a finite density of states for spinon excitations, but the spin structure factor of this state does not necessarily peak at any commensurate wave vector. Moreover, after the system develops a weak spin-density wave, the spinon Fermi-surface is not immediately gapped, and the system still has a finite density of states for gapless spinons. These predictions are not completely consistent with our inelastic neutron data.

(ii) A quantum critical state between Z_2 spin liquid and an ordered state with commensurate spiral spin density wave [28]. This quantum critical state has gapless spinon excitations, and its spin structure factor indeed peaks at momenta Q_0 .

(iii) A gapless spin-liquid state with both Dirac-like fermionic spinon excitations, and spinon excitations with a quadratic band touching. This is a stable gapless spin-liquid state whose spin structure factor peaks at Q_0 . In Ref. [29], this spin-liquid state was proposed for the spin-1 material $\text{Ba}_3\text{NiSb}_2\text{O}_9$, but the proposal is equally valid for the spin-1/2 case after a simple generalization [30].

Based on these observations we conclude that the theories (ii) and (iii) are better candidates for the spin liquid state that is responsible for the fractionalization of spin-wave excitations in $\text{Ba}_3\text{CoSb}_2\text{O}_9$.

In summary, single crystals of $\text{Ba}_3\text{CoSb}_2\text{O}_9$, a 2D $S = 1/2$ triangular-lattice antiferromagnet, were synthesized. In a magnetic field applied along the magnetic easy axis, the c axis, the system undergoes successive magnetic phase transitions with a uud phase stabilized even at 27 mK. Although $\text{Ba}_3\text{CoSb}_2\text{O}_9$ orders at about 3.7 K, we argue, based on the extended continuum observed above the spin-wave excitations at 1.5 K, that it is in close proximity to a spin-liquid phase. These results make $\text{Ba}_3\text{CoSb}_2\text{O}_9$ a rare spin-1/2 triangular-lattice magnet in which not only the uud phase is stabilized but also spin waves may be fractionalized.

We thank H. Tanaka for communicating part of the results of Ref. 14 prior to publication. C. X. is supported by the Sloan Foundation. A. M. H. acknowledges the support of NSERC. H. J. S. acknowledges the Vanier program and UMGF. C. R. W. acknowledges support through NSERC, CFI, and the ACS Petroleum Fund. I. U. was supported by the Global CEO Program

“Nanoscience and Quantum Physics” at Tokyo Tech, funded by the Ministry of Education, Culture, Sports, Science, and Technology of Japan. This work utilized facilities supported in part by the National Science Foundation under Agreement No. DMR-0944772. The magnetic and calorimetric measurements were performed at the National High Field Magnet Laboratory, which is supported by NSF-DMR-0654118 and the State of Florida. The work at ORNL was supported by the U.S. Department of Energy, Basic Energy Sciences, Materials Sciences and Engineering Division.

* Electronic address: hzhou10@utk.edu

- [1] L. Balents, *Nature* **464**, 199 (2010).
- [2] P. W. Anderson, *Mater. Res. Bull.* **8**, 153 (1973).
- [3] S. Yamashita, Y. Nakazawa, M. Oguni, Y. Oshima, H. Nojiri, Y. Shimizu, K. Miyagawa, and K. Kanoda, *Nature Phys.* **4**, 459 (2008).
- [4] M. Yamashita, N. Nakata, Y. Kasahara, T. Sasaki, N. Yoneyama, N. Kobayashi, S. Fujimoto, T. Shibauchi, and Y. Matsuda, *Nature Phys.* **5**, 44 (2009).
- [5] M. Yamashita, N. Nakata, Y. Senshu, M. Nagata, H. M. Yamamoto, R. Kato, T. Shibauchi, and Y. Matsuda, *Science* **328**, 1246 (2010).
- [6] T. Itou, A. Oyamada, S. Maegawa, and R. Kato, *Nature Phys.* **6**, 673 (2010).
- [7] R. Coldea, D. A. Tennant, A. M. Tsvelik, and Z. Tylczynski, *Phys. Rev. Lett.* **86**, 1335 (2001).
- [8] R. Coldea, D. A. Tennant, and Z. Tylczynski, *Phys. Rev. B* **68**, 134424 (2003).
- [9] A. V. Chubukov and D. I. Golosov, *J. Phys.: Condens. Matter* **3**, 69 (1991).
- [10] S. Miyahara, K. Ogino, and N. Furukawa, *Physica (Amsterdam)* **378B-380B**, 587 (2006).
- [11] J. Alicea, A. V. Chubukov, and O. A. Starykh, *Phys. Rev. Lett.* **102**, 137201 (2009).
- [12] T. Ono, H. Tanaka, H. Aruga Katori, F. Ishikawa, H. Mitamura, and T. Goto, *Phys. Rev. B* **67**, 104431 (2003).
- [13] N. A. Fortune, S. T. Hannahs, Y. Yoshida, T. E. Sherline, T. Ono, H. Tanaka, and Y. Takano, *Phys. Rev. Lett.* **102**, 257201 (2009).
- [14] Y. Shirata, H. Tanaka, A. Matsuo, and K. Kindo, *Phys. Rev. Lett.* **108**, 057205 (2012).
- [15] Y. Doi, Y. Hinatsu, and K. Ohoyama, *J. Phys.: Condens. Matter* **16**, 8923 (2004).
- [16] S. Miyashita and H. Kawamura, *J. Phys. Soc. Jpn.* **54**, 3385 (1985).
- [17] S. Miyashita, *J. Phys. Soc. Jpn.* **55**, 3605 (1986).
- [18] P.-É. Melchy and M. E. Zhitomirsky, *Phys. Rev. B* **80**, 064411 (2009).
- [19] H. Kawamura and S. Miyashita, *J. Phys. Soc. Jpn.* **54**, 4530 (1985).
- [20] M. V. Gvozdikova, P.-E. Melchy, and M. E. Zhitomirsky, *J. Phys.: Condens. Matter* **23**, 164209 (2011).
- [21] L. Seabra, T. Momoi, P. Sindzingir, and N. Shannon, *Phys. Rev. B* **84**, 214418 (2011).
- [22] R. Ishii, S. Tanaka, K. Onuma, Y. Nambu, M. Tokunaga, T. Sakakibara, N. Kawashima, Y. Maeno, C. Broholm, D. P. Gautreaux, J. Y. Chan, and S. Nakatsuji, *Euro. Phys. Lett.* **94**, 17001 (2011).
- [23] A. Honecker, *J. Phys.: Condens. Matter* **11**, 4697 (1999).
- [24] D. J. J. Farnell, R. Zinke, J. Schulenburg, and J. Richter, *J. Phys.: Condens. Matter* **21**, 406002 (2009).
- [25] T. Sakai and H. Nakano, *Phys. Rev. B* **83**, 100405(R) (2011).
- [26] S. S. Lee, P. A. Lee, and T. Senthil, *Phys. Rev. Lett.* **98**, 067006 (2007).
- [27] Y. Zhou and P. A. Lee, *Phys. Rev. Lett.* **106**, 056402 (2011).
- [28] Y. Qi, C. Xu, and S. Sachdev, *Phys. Rev. Lett.* **102**, 176401 (2009).
- [29] C. Xu, F. Wang, Y. Qi, L. Balents, and M. P. A. Fisher, *Phys. Rev. Lett.* **108**, 087204 (2012).
- [30] E. G. Moon and C. Xu, in preparation.